High physiological thermal triplex stability optimization of twisted intercalating nucleic acids (TINA)†

Niels Bomholt, Amany M. A. Osman‡ and Erik B. Pedersen*

Received 21st May 2008, Accepted 30th June 2008
First published as an Advance Article on the web 6th August 2008
DOI: 10.1039/b808564a

The structure of the monomer (*R*)-1-*O*-[4-(1-pyrenylethynyl)phenylmethyl]glycerol (**1**) in twisted intercalating nucleic acids (TINA) was optimized for stabilizing interactions between the intercalator and surrounding nucleobases when used as a triplex forming oligonucleotide (TFO). Enhancement of π–π interactions with nucleobases of the TFO was achieved by increasing the aromatic surface using the (*R*)-1-*O*-[4-(1-pyrenylethynyl)naphthylmethyl]glycerol monomer (**2**). Bulge insertion of **2** in the middle of a Hoogsteen-type triplex increased the triplex thermal stability, $\Delta T_m = +2.0$ °C compared with **1** at pH 7.2. Syntheses and thermal denaturation studies of triplexes and duplexes are described for three novel TINA monomers. The influence of π–π interactions, link length and the positioning of the ether in the linker in the TINA derivatives are described.

Introduction

Triplex forming oligonucleotides (TFOs) are cable of targeting DNA duplexes through sequence specific recognition, making the antigene technology a potential tool for human gene therapy and diagnostics applications.[1,2] Triplex formation results from purines' ability to form additional hydrogen bonds to a third oligonucleotide positioned in the major groove of the DNA duplex.[3] These so called Hoogsteen hydrogen bonds are specifically formed between G·G × C and A·A × T or T·A × T and C^+·G × C. In the former case, the triplex is known as a reverse-Hoogsteen triplex or as an antiparallel triplex, with an antiparallel binding motif. The latter case is known as a Hoogsteen triplex or as a parallel triplex, with a parallel binding motif. In both cases, the triplex formation is limited by the need of a duplex target containing a homopurine tract of ideally 15–30 nucleobases.[4] In addition, the parallel triplex is limited by the requirement of N3 protonation of cytosine in order to form the C^+·G × C triplet, rendering the parallel triplex unstable at physiological pH.[5] Several modified nucleotides have in recent years successfully been applied to the triplex technology, in order to overcome low thermal stability and to improve targeting, such as locked nucleic acids (LNA),[6] 5′–5′-linked intercalating alternate strand TFOs[7,8] and modified nucleotides with the ability to recognize all four base pairs.[9] Insertion of conjugated intercalators in the TFO have been shown to be an effective way to stabilize triplexes. The twisted intercalating nucleic acids (TINA) inserted as a bulge in a triple-helix forming oligonucleotide (TFO), stabilize parallel Hoogsteen triplexes considerably, with $\Delta T_m = +19.0$ °C for the insertion of one (*R*)-1-*O*-[4-(1-pyrenylethynyl)phenylmethyl]glycerol monomer (**1**) in a 14-mer TFO.[10] High thermal stability was not achieved at the expense of low mismatch discrimination as a single base pair mismatch in the dsDNA resulted in a minimum ΔT_m of –11.5 °C. Moreover, the Watson–Crick duplex was destabilized, demonstrating discrimination between parallel duplex/triplex and antiparallel duplex. In addition, Paramavisam *et al.*[11] have recently shown that incorporation of TINA monomers in G-rich oligonucleotides interferes with quadruplex formation at physiologic potassium concentrations releasing the oligonucleotide for antiparallel triplex formation. These properties make the TINA monomer a suitable tool for dsDNA targeting in silencing and in diagnostic applications.

In our ongoing research, optimization of the thermal triplex stability by intercalation has mainly been focused on modifying the 1-pyrenylethynyl moiety. Replacing this moiety with 9-aminoacridin-2-ylethynyl,[12] naphthalen-1-ylethynyl, biphenyl-4-ethynyl, phenyl-1-ethynyl[13] or 4-(1-(pyren-1-yl)-1*H*-1,2,3-triazol-4-yl)[14] all resulted in lower thermal stability indicating that the 4-(1-pyrenylethynyl) moiety has an appropriate size and configuration for optimal intercalation. It is worth mentioning that we have recently shown that by substituting pyrene with a naphthalimide comprising an *N*,*N*-dimethylaminoethyl group, the triplex stability can be increased as a result of an ionic interaction between the protonated dimethylamino group and the negatively charged phosphate backbone of the duplex.[15]

Herein we report a thermal stability optimization of TINA (**1**) based on a molecular modelling examination of its intercalating properties, leading to a $\Delta T_{m(pH7.2)} = +2.0$ °C for (*R*)-1-*O*-[4-(1-pyrenylethynyl)naphthylmethyl]glycerol (**2**) where the benzene ring has been substituted by naphthalene (Fig. 1). Length dependence of the glycerol for the optimized TINA was investigated using the analogues (*S*)-[4-(1-pyrenylethynyl)naphthylmethoxy]butane-1,2-diol (**3**). Furthermore was the importance of the ether position in the linker with respect to thermal stability investigated by the synthesis of a third novel TINA, (*S*)-4-(4-(pyren-1-ylethynyl)phenoxy)butane-1,2-diol (**4**).

Nucleic Acid Center, Department of Physics and Chemistry, University of Southern Denmark, Campusvej 55, DK-5230, Odense M, Denmark

† Electronic supplementary information (ESI) available: Melting curves of thermal denaturation experiments of triplexes **ON1**–**ON5/D2** and **ON6**–**ON10/D2**; first derivative plots of thermal denaturation experiments of triplexes **ON1**–**ON5/D2** and **ON6**–**ON10/D2**; HPLC ion-exchange chromatography and purity determination of **ON3**, **ON4**, **ON5**, **ON7**, **ON8**, **ON9** and **ON10**. See DOI: 10.1039/b808564a

‡ On leave from Chemistry Department, Faculty of Science, Menoufia University, Shebin El-Koam, Egypt.

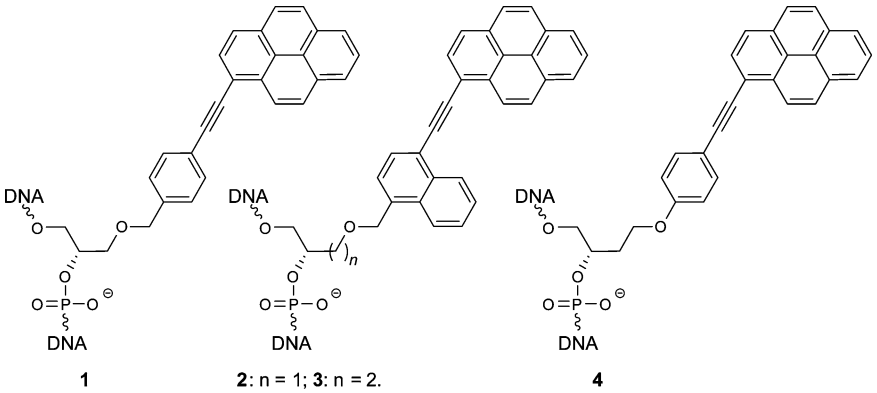

Fig. 1 Twisted intercalating nucleic acids.

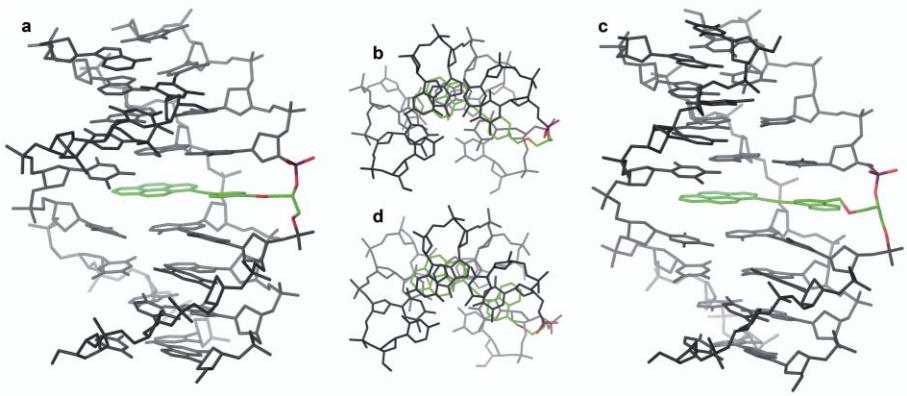

Fig. 2 Representative low-energy structures of the truncated triplexes obtained by molecular modelling. The monomer TINA **1** (Fig. 2a and 2b) and **2** (Fig. 2c and 2d) are shown in colour. The side view is shown on Fig. 2a and 2c. The top view is shown on Fig. 2b and 2d.

Results and discussion

Molecular modelling

In order to optimize the intercalating properties of the TINA (**1**), we decided to examine it *via* molecular modelling studies. An AMBER* force field was used to generate representative low-energy structures of a truncated 8mer triplex with the bulge insertion of the monomer (Fig. 2).

As can be seen from Fig. 2a and 2b, the pyrene is positioned in the Watson–Crick duplex where it forms π–π interactions to the adjacent nucleobases. The C–C triple bond is believed to enhance intercalating properties,[16] which is supported by this study, where it is positioned within 3.5 Å to neighbouring nucleobases, allowing it to form stabilizing π–π interactions. In addition, the ability of twisting the aromatic moieties around the triple bond allows them to adjust to the local secondary structure of the triplex. The pyrene ring is positioned in the duplex whereas the benzene ring interacts with the two adjacent nucleobases of the TFO by π–π interactions, adding to the triplex stability. In addition, it ensures the same degree of enforced unwinding of the TFO as for the duplex and consequently ensures accurate T·A × T and C^+·G × C triplets neighbouring the bulge insertion. Previous optimization studies have, as mentioned earlier, failed to enhance triplex stability at physiological pH by substituting the pyrene moiety with different aromatic systems as well as substituting the acetylene bond with a 1,2,3-triazole. Until now, the importance of the benzene ring has not been investigated. Our modelling study showed that the benzene ring could be substituted with naphthalene as shown in Fig. 2c and 2d. As a consequence of the larger aromatic surface, the naphthalene moiety will be able to obtain more favourable π–π interactions with the nucleobases of the TFO and thereby enhance triplex stability at elevated temperatures. The second conformation of the unsymmetrical intercalator where the naphthalene is twisted 180° around the triple bond results in equal interacting properties and no optimal conformation could be assigned.

Synthesis of TINA phosphoramidites

In addition to the planned synthesis of **2**, we wanted to investigate the effect of increasing the linkage length by synthesizing a second TINA analogue **3** with an extra carbon atom in the linkage between the TFO backbone and the intercalator comprising naphthalene and pyrene. **2** and **3** were synthesized from the enantiomeric pure starting compounds **5** and **6** (Scheme 1), respectively, which were reacted with 1-bromo-4-(bromomethyl)naphthalene[7] under Dean–Stark conditions (toluene, KOH), followed by the deprotection of the isopropylidene groups in 80% aq. AcOH to afford **7** and **8** without using chromatography in satisfactory purity for the subsequent step. The Sonogashira coupling with 1-ethynylpyrene was done with $Pd(PPh_3)_2Cl_2$, CuI, PPh_3, NEt_3, reflux under Ar resulting in compounds **9** and **10** in 47% and 80% yield, respectively. The primary hydroxy groups were protected with DMT-Cl

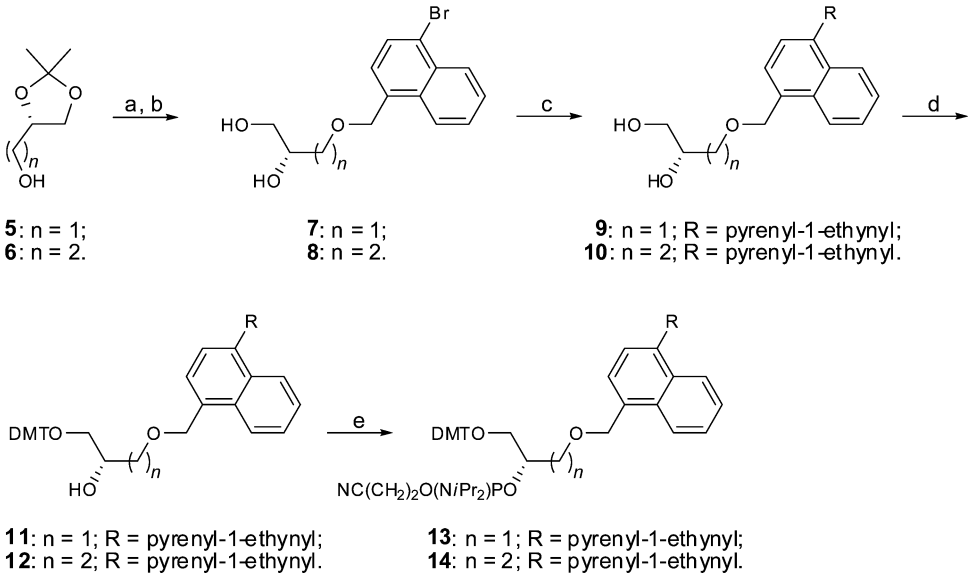

Scheme 1 *Reagents and conditions:* (a) 1-bromo-4-(bromomethyl)naphthalene,[7] KOH, toluene, reflux; (b) 80% aq. AcOH, room temperature; (c) 1-ethynylpyrene, $Pd(PPh_3)_2Cl_2$, CuI, PPh_3, NEt_3, reflux, Ar; (d) DMTCl, pyridine, room temperature; (e) 2-cyanoethyl-*N*,*N*,*N*′,*N*′-tetraisopropylphosphordiamidite, diisopropylammonium tetrazolide, CH_2Cl_2, 0 °C → room temperature.

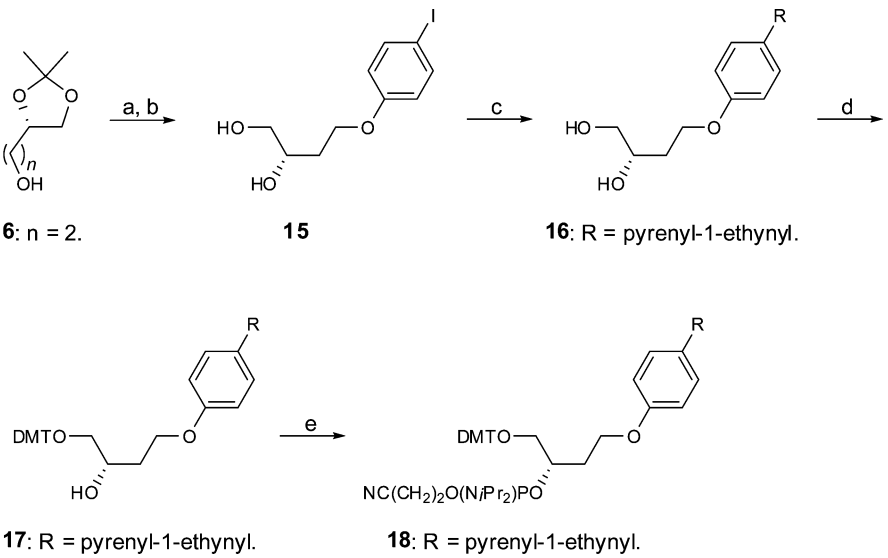

Scheme 2 *Reagents and conditions:* (a) 4-iodophenol, DEAD, PPh_3, THF, 0 °C → room temperature; (b) 80% aq. AcOH, room temperature; (c) 1-ethynylpyrene, $Pd(PPh_3)_2Cl_2$, CuI, NEt_3, room temperature, Ar; (d) DMTCl, pyridine, room temperature; (e) 2-cyanoethyl-*N*,*N*,*N*′,*N*′-tetraisopropylphosphordiamidite, diisopropylammonium tetrazolide, CH_2Cl_2, 0 °C → room temperature.

in dry pyridine to give **11** and **12**, before they were converted to the respective phosphoramidites, **13** and **14**, by treatment with 2-cyanoethyl-*N*,*N*,*N*′,*N*′-tetraisopropylphosphordiamidite and diisopropylammonium tetrazolide in dry CH_2Cl_2, which were used in standard DNA synthesis.

To find the best TINA derivative, a third novel TINA derivative **4** was synthesized. Here the purpose was to investigate the importance of the ether position in the linkage with respect to thermal stability of the corresponding DNA triplexes. Compound **4** was synthesized from compound **6** (Scheme 2), which was reacted with 4-iodophenol under Mitsunobu conditions, followed by the deprotection of the isopropylidene groups in 80% aq. AcOH, affording **15** in satisfactory yield. The subsequent Sonogashira coupling with 1-ethynylpyrene, $Pd(PPh_3)_2Cl_2$, CuI, NEt_3 under Ar afforded **16** in 73% yield. After protection of the primary hydroxy group with DMT-Cl in dry pyridine to give **17**, the corresponding phosphoramidite **18** could be isolated after treatment with 2-cyanoethyl-*N*,*N*,*N*′,*N*′-tetraisopropylphosphordiamidite and diisopropylammonium tetrazolide in dry CH_2Cl_2 and it could subsequently be used for standard DNA synthesis.

Thermal stability studies

The phosphoramidites, **13**, **14** and **18**, were used in standard DNA synthesis to obtain modified oligonucleotides possessing TINAs, which were used in pH dependent thermal stability studies of the Hoogsteen-type triplex as well as parallel and antiparallel

Table 1 T_m [°C] data for DNA triplex, parallel and antiparallel duplex melting, taken from UV melting curves ($\lambda = 260$ nm)

		Triplex[a]		Parallel duplex[b]	Antiparallel duplex[b]	
		3′-CTGCCCCTTTCTTTTTT 5′-GACGGGGAAAGAAAAAA (duplex **D1**)		5′-GACGGGGAAAGAAAAAA (ssDNA **ON17**)	3′-GGGGAAAGAAAAAA (ssDNA **ON18**)	
Entry	Sequence	pH 6.0 T_m/°C	pH 7.2 T_m/°C	pH 6.0 T_m/°C	pH 6.0 T_m/°C	pH 7.2 T_m/°C
ON1[c]	5′-CCCCTTTCTTTTTT	27.0[e](26.5)[d]	<5.0[e]	19.0[c]	48.0[c]	47.0[c]
ON2[c]	5′-CCCCTT**1**TCTTTTTT	45.5(44.0)[d]	28.0[e]	33.5[c]	46.5[c]	45.5[c]
ON3	5′-CCCCTT**2**TCTTTTTT	48.0[e](46.5)[d]	30.0	36.0	46.0	47.0
ON4	5′-CCCCTT**3**TCTTTTTT	42.5(40.5)[d]	24.5	29.5	48.0	48.0
ON5	5′-CCCCTT**4**TCTTTTTT	45.5(42.5)[d]	27.0	31.0	47.5	48.0
ON6[c]	5′-CCCCTT**1**TCT**1**TTTTT	56.5[e](51.0)[d]	40.0[e]	38.0[c]	45.0[c]	42.0[c]
ON7	5′-CCCCTT**2**TCT**2**TTTTT	58.5[f](59.5)[d]	*n.t.*[g]	41.5	42.5	39.5
ON8	5′-CCCCTT**3**TCT**3**TTTTT	50.5[e](49.5)[d]	*n.t.*[g]	33.0	38.5	40.0
ON9	5′-CCCCTT**4**TCT**4**TTTTT	57.0[f](54.0)[d]	42.0	39.0	44.0	43.0
ON10	5′-CCCCT**2**TTCTT**2**TTTT	58.5[f](62.5)[d,e,h]	46.5[e,h]	41.5	45.0	43.5

[a] $C = 1.5$ μM of **ON1–ON10** and 1.0 μM of each strand of dsDNA in 20 mM sodium cacodylate, 100 mM NaCl, 10 mM $MgCl_2$, pH 6.0 and 7.2; duplex $T_m = 57.5$ °C and 58.0 °C at pH 6.0 and pH 7.2 respectively. [b] $C = 1.0$ μM of each strand in 20 mM sodium cacodylate, 100 mM NaCl, 10 mM $MgCl_2$, pH 6.0 and pH 7.2. [c] Oligonucleotides and T_m data are from ref. 10. [d] T_m was determined with the extended duplex **D2**: 3′-CCGGCTGCCCCTTTCTTTTTTCGCG/5′-GGCCGACGGGGAAAGAAAAAAGCGC, the target being underlined, duplex $T_m = 74.0$ °C. [e] Third strand and duplex melting overlapped. [f] Third strand and duplex melting overlaid. [g] *n.t.* = no transition observed. [h] Transition determined at 373 nm.

Table 2 T_m [°C] data for mismatched triplex melting, taken from UV melting curves ($\lambda = 260$ nm)

		Triplex[a]			
		3′-CTGCCCCTT**X**CTTTTTT 5′-GACGGGGAA**Y**GAAAAAA			
		Duplex **D1**	Duplex **D3**	Duplex **D4**	Duplex **D5**
Entry	Sequence	**X·Y = T·A**	**X·Y = A·T**	**X·Y = C·G**	**X·Y = G·C**
ON1[b]	5′-CCCCTTTCTTTTTT	27.0	< 5.0	< 5.0	< 5.0
ON2[b]	5′-CCCCTT**1**TCTTTTTT	45.5	27.0	34.5	28.5
ON3	5′-CCCCTT**2**TCTTTTTT	48.0[c]	28.5	35.5	28.0
ON4	5′-CCCCTT**3**TCTTTTTT	42.5	26.5	28.0	25.0
ON5	5′-CCCCTT**4**TCTTTTTT	45.5	32.5	40.0	31.5

[a] $C = 1.5$ μM of **ON1–ON5** and 1.0 μM of each strand of dsDNA in 20 mM sodium cacodylate, 100 mM NaCl, 10 mM $MgCl_2$, pH 6.0. [b] Oligonucleotides and T_m data are from ref. 10. [c] See Table 1.

duplexes. For comparison, the modified oligonucleotides and their complementary strands used in this study are equal to those described earlier for other TINA analogues.[10,12–15] Thermal stability of triplexes and duplexes were assessed by thermal denaturation experiments, and the melting temperatures (T_m, °C) were determined from melting curves *via* the first derivation method (Tables 1, 2 and ESI†).[17] Due to high triplex stability for **ON3/D1** with the bulge insertion of **2** in the middle of the TFO, an overlap of triplex and duplex melting curves was observed, precluding an accurate T_m determination. Similar overlaps were observed for the bulge insertion of two TINA-analogues, therefore, in order to assess accurate and comparable T_m's at pH 6.0 for triplexes formed by **ON2–ON10**, an extended target duplex **D2** was used. Thermal melting measurements using an extended target duplex resulted in higher T_m of the duplex, allowing a non-overlapping transition of the triplex, thereby ensuring an accurate T_m-determination. But in the case of **ON10**, even the triplex transition overlapped with the duplex **D2**, for which the absorbance for the monomer **2** (373 nm) was used to determine the transition. From these measurements, it was possible to determine T_m for all triplexes (**ON1–ON10/D2**) at pH 6.0 and compare stabilizing properties of the novel TINA analogues.

The highest thermal stability at pH 6.0 was observed for **ON3/D2** ($\Delta T_m = +2.5$ °C compared to **ON2/D2**) with a $T_m = 46.5$ °C and a ΔT_m/mod = +20.0 °C. In addition, the length of the glycerol linkage was shown to be optimal for obtaining high thermal stability, since a $\Delta T_m = -5.5$ °C at pH 6.0 was observed for **ON4/D2** when compared to **ON3/D2**. The position of the ether in TINA was shown only to influence the triplex stability mildly, since **ON5/D2** showed similar T_m as **ON2/D2** at both pH values. At pH 7.2, an overall decrease in thermal stability was observed due to the lack of cytosine protonation, but triplexes formed by **ON3–ON5** showed a similar distribution in thermal stability as observed at pH 6.0 with a maximum thermal stability for **ON3/D1**, $T_m = 30.0$ °C. This enhanced triplex stability at both pH values proves that the larger aromatic surface of the naphthalene moiety of TINA **2** improves, pH-independently, π–π interactions with neighbouring nucleobases of the TFO as compared to the smaller aromatic surface of the benzene ring of TINA **1**.

Upon bulge insertion of two TINA monomers in the TFO, the triplex stability at pH 6.0 was further enhanced (**ON6–ON9/D2**) with a ΔT_m/mod = +16.5 °C for the **ON7/D2** triplex compared to ΔT_m/mod = +12.3 °C for the **ON6/D2**. Surprisingly, no triplex formation was detected for **ON7–ON8/D1** at pH 7.2. This observation could be the result of deprotonation of the cytosine residues, making it more difficult to accommodate two large inserted intercalators in a stringent triplex structure. The size of the intercalator in the case of **ON7–8** is larger than for **ON6** and **ON9** because of the naphthalene moiety, explaining why this behaviour was only observed for these TFOs.

In order to investigate whether the promising analogue **2** at pH 7.2 could achieve a sufficiently relaxed triplex structure, the oligonucleotide **ON10** was synthesized with increased distance between the bulge insertions. As can be seen from Table 1, **ON10** resulted in a small increase in thermal stability at pH 6.0 (ΔT_m = +3.5 °C) when compared to **ON7/D2**, but more importantly, triplex formation was observed at pH 7.2 with a thermal stability of 46.5 °C allowing the use of multiple insertion of the optimized TINA analogue **2** at physiological pH.

An important property of TINAs is their ability to favour Hoogsteen hybridization over Watson–Crick. This is also the case for the bulge insertion of the analogues **2**, **3** and **4** in the parallel duplex (**ON17**), which results in stabilization, whereas the antiparallel duplex (**ON18**), is only mildly stabilized or destabilized.

High sensitivity to mismatches is essential for the use of selective TFOs in the triplex technology. Therefore the thermal stability of **ON3–ON5** towards a single neighbouring mismatch in the purine strand was investigated, Table 2. In all cases the triplex were destabilized with ΔT_m in the range of –14.0 to –21.5 °C. Surprisingly **ON4** showed less significant mismatch sensitivity compared to **ON2**, even though they gave similar thermal stability of matched triplexes and duplexes. **ON3** mismatch sensitivity was not affected even though an increased triplex stability was observed for the matched triplex.

Conclusions

It was found possible to improve the lead structure (*R*)-1-*O*-[4-(1-pyrenyl-ethynyl)phenylmethyl]glycerol monomer (**1**) by optimizing the stabilizing interactions between the intercalator and the surrounding nucleobases in a DNA triplex. The molecular modelling study showed that increasing the aromatic surface of the intercalator moiety between TFO nucleobases could enhance π–π interactions thereby increasing the thermal stability of the triplex. In addition to the synthesis of the novel TINA analogue **2** based on the molecular modelling study, importance of the linkage length and ether position in the linkage was investigated by the synthesis of the two novel TINA analogues **3** and **4**. Bulge insertion of the (*R*)-1-*O*-[4-(1-pyrenylethynyl)naphthylmethyl]glycerol monomer (**2**) gave the best results and it increased the triplex thermal stability, ΔT_m = +2.0 °C at pH 7.2, when compared with **1**, thereby showing the correlation of π–π interactions of an intercalator and thermal stability. The novel TINA analogues **3** and **4** showed that the glycerol linkage has an optimal length and that no significant importance of the ether position could be observed. Insertion of two monomers (**2**), three nucleobases apart, **ON7**, led to further increase of thermal stability at pH 6.0 compared with **1**, whereas no triplex formation was observed at pH 7.2. However, when the distance between the insertions of **2** was increased to five nucleobases (**ON10**), the triplex formation was observed at physiological pH 7.2.

Experimental section

General

NMR spectra were recorded on a Varian Gemini 2000 spectrometer; ^{1}H at 300 MHz, ^{13}C at 75 MHz and ^{31}P at 121.5 MHz. The internal standard used in ^{1}H NMR was TMS (δ = 0.00) for $CDCl_3$ and DMSO-d_6; in ^{13}C NMR was $CDCl_3$ (δ = 77.16) and DMSO-d_6 (δ = 39.52); in ^{31}P NMR was H_3PO_4 (δ = 0.00) used as external standard. Accurate ion mass determinations were performed using the 4.7 Tesla Ultima Fourier Transform (FT) mass spectrometer (Ion Spec, Irvine, CA). The $[M]^+$ ions were peak matched using ions derived from the 2,5-dihydroxybenzoic acid matrix. EI-MS was performed on Finnigan SSQ 710. Melting points were detected with a Büchi melting point apparatus. Thin layer chromatography (TLC) analyses were carried out with use of TLC plates 60 F_{254} purchased from Merck and visualized under an UV light (254 nm). The silica gel (0.040–0.063 mm) used for column chromatography was purchased from Merck. Solvents used for column chromatography and reagents were used as purchased without further purification.

Molecular modelling

Molecular modelling was performed with a MacroModel v9.1 from Schrödinger. All calculations were conducted with an AMBER* force field and the GB/SA water model. The dynamic simulations were preformed with stochastic dynamics, a SHAKE algorithm to constrain bonds to hydrogen, time step of 1.5 fs and simulation temperature of 300 K. Simulation for 0.5 ns with an equilibration time of 150 ps generated 250 structures, which all were minimized using the PRCG method with a convergence threshold of 0.05 kJ mol^{-1}. The minimized structures were examined with Xcluster from Schrödinger, and representative low-energy structures were selected. The starting structures were generated with Insight II v97.2 from MSI, followed by incorporation of the modified nucleotide.

Synthesis

(*R*)-3-((4-Bromonaphthalen-1-yl)methoxy)propane-1,2-diol 7. (*S*)-(+)-2,2-Dimethyl-1,3-dioxolane-4-methanol (**5**; 2.33 g, 17.63 mmol) and 1-bromo-4-(bromomethyl)naphthalene[7] (5.00 g, 16.67 mmol) were refluxed under Dean–Stark conditions in toluene (150 mL) in the presence of KOH (17.11 g, 304.9 mmol) for 21 h. The reaction mixture was allowed to cool, and H_2O (60 mL) was added. After separation of the phases, the water layer was washed with toluene (2 × 30 mL). Combined organic layers were washed with H_2O (30 mL) and concentrated under reduced pressure to afford (*S*)-4-(((4-bromonaphthalen-1-yl)methoxy)methyl)-2,2-dimethyl-1,3-dioxolane as a reddish brown oil, which was used in the next step without further purification. Yield 4.40 g (88%). ^{1}H NMR ($CDCl_3$) δ 1.35, 1.41 (2 × s, 6H, 2 × C(CH_3)$_2$), 3.56 (m, 2H, ArCH$_2$OCH_2), 3.70 (m, 1H, CHCH_2O), 4.01 (m, 1H, CHCH_2O), 4.28 (quintet, J = 6.0 Hz, 1H,

CH_2CHCH_2), 4.93, 5.02 (2 × d, J = 12.6 Hz, 2H, $ArCH_2O$), 7.33, 7.73 (2 × d, J = 7.8 Hz, 2H, Ar), 7.57–7.61 (m, 2H, Ar), 8.09–8.12 (m, 1H, Ar), 8.27–8.30 (m, 1H, Ar). ^{13}C NMR ($CDCl_3$) δ 25.5, 26.9 (2 × $C(CH_3)_2$), 66.9 ($CHCH_2O$), 71.2 (OCH_2CH), 71.8 ($ArCH_2O$), 74.8 (CH_2CHCH_2), 109.6 ($C(CH_3)_2$), 123.6, 124.6, 127.0, 127,2, 127.4, 127.9, 129.4, 132.2, 132.9, 133.6 (Ar). HR-MALDI-MS calcd for $C_{17}H_{19}BrO_3Na$ $[M + Na]^+$ m/z 373.0410; found m/z 373.0397. (*S*)-4-(((4-Bromonaphthalen-1-yl)methoxy)methyl)-2,2-dimethyl-1,3-dioxolane (4.40 g, 12.53 mmol) was treated with 80% aq. AcOH (40 mL) for 48 h at room temperature. The solvent was removed under reduced pressure and the residue was coevaporated with toluene–EtOH (2 × 60 mL, 5 : 1, v/v). The residue was dried under reduced pressure to afford **7** as brown oil, which was used in the next step without further purification. Yield 3.52 g (80%). ^{1}H NMR ($CDCl_3$) δ 3.56–3.69 (m, 5H, OCH_2CHCH_2OH), 4.21 (br. s, 2H, 2 × OH), 4.94 (s, 2H, $ArCH_2O$), 7.30, 7.73 (2 × d, J = 7.8 Hz, 2H, Ar), 7.58–7.62 (m, 2H, Ar), 8.05–8.08 (m, 1H, Ar), 8.27–8.31 (m, 1H, Ar). ^{13}C NMR ($CDCl_3$) δ 64.0 ($CHCH_2OH$), 70.8 ($CHCH_2OH$), 71.8 (CH_2CHCH_2, $ArCH_2O$), 123.8, 124.3, 127.2, 127.3, 127.5, 128.0, 129.4, 132.3, 133.0, 133.3 (Ar). HR-MALDI-MS calcd for $C_{14}H_{15}BrO_3Na$ $[M + Na]^+$ m/z 333.0097; found m/z 333.0085.

(*S*)-4-((4-Bromonaphthalen-1-yl)methoxy)butane-1,2-diol 8. (*S*)-4-(2-((4-Bromonaphthalen-1-yl)methoxy)ethyl)-2,2-dimethyl-1,3-dioxolane was synthesized from (*S*)-(+)-4-(2-hydroxyethyl)-2,2-dimethyl-1,3-dioxolane (**6**) according to the procedure described under **7**. Yield 75% reddish brown oil. ^{1}H NMR ($CDCl_3$) δ 1.33, 1.39 (s, 6H, 2 × $C(CH_3)_2$), 1.84–1.91 (m, 2H, OCH_2CH_2), 3.53 (m, 1H, $CHCH_2O$), 3.65 (m, 2H, OCH_2CH_2), 4.00 (m, 1H, $CHCH_2O$), 4.19 (m, 1H, CH_2CHCH_2), 4.85–4.94 (m, 2H, $ArCH_2$), 7.32, 7.73 (2 × d, J = 7.8 Hz, 2H, Ar), 7.56–7.63 (m, 2H, Ar), 8.06–8.09 (m, 1H, Ar), 8.27–8.30 (m, 1H, Ar). ^{13}C NMR ($CDCl_3$) δ 25.9, 27.1 (2 × $C(CH_3)_2$), 34.0 (OCH_2CH_2), 67.4 ($CHCH_2O$), 69.7 (OCH_2CH_2), 71.4 ($ArCH_2O$), 73.9 (CH_2CHCH_2), 108.7 ($C(CH_3)_2$), 123.4, 124.5, 127.0, 127,1, 127.3, 127.9, 129.4, 132.2, 133.0, 134.0 (Ar). HR-MALDI-MS calcd for $C_{18}H_{21}BrO_3Na$ $[M + Na]^+$ m/z 387.0566; found m/z 387.0577. Compound **8** was synthesized from (*S*)-4-(2-((4-bromonaphthalen-1-yl)methoxy)ethyl)-2,2-dimethyl-1,3-dioxolane according to the procedure described for **7**. Yield 100% brown oil. ^{1}H NMR ($CDCl_3$) δ 1.72–1.77 (m, 2H, OCH_2CH_2), 3.40–3.46 (m, 1H, $CHCH_2O$), 3.55–3.60 (m, 1H, $CHCH_2O$), 3.68–3.73 (m, 2H, OCH_2CH_2), 3.85–4.01 (m, 1H, CH_2CHCH_2), 4.01 (s, 2H, 2 × OH), 4.86–4.94 (m, 2H, $ArCH_2$), 7.30, 7.72 (2 × d, J = 7.50 Hz, 2H, Ar), 7.57–7.61 (m, 2H, Ar), 8.03–8.06 (m, 1H, Ar), 8.26–8.29 (m, 1H, Ar). ^{13}C NMR ($CDCl_3$) δ 32.9 (OCH_2CH_2), 66.7 (OCH_2CH_2), 68.3 ($CHCH_2OH$), 71.1 ($CHCH_2OH$), 71.5 ($ArCH_2O$), 123.6, 124.3, 126.9, 127.1, 127.3, 128.0, 129.2, 132.2, 132.9, 133.5 (Ar). HR-MALDI-MS calcd for $C_{15}H_{17}BrO_3Na$ $[M + Na]^+$ m/z 347.0253; found m/z 347.0267.

(*R*)-3-((4-(Pyren-1-ylethynyl)naphthalen-1-yl)methoxy)propane-1,2-diol 9. (*R*)-3-((4-Bromo-naphthalen-1-yl)methoxy)propane-1,2-diol (**7**; 1.01 g, 3.25 mmol), $Pd(PPh_3)_2Cl_2$ (158 mg, 0.23 mmol), CuI (73 mg, 0.38 mmol) and powdered PPh_3 (169 mg, 0.64 mmol) were dissolved in dry NEt_3 (40 mL). The reaction mixture was flushed with Ar before 1-ethynylpyrene (1.09 g, 4.82 mmol) was added. The reaction mixture was stirred under reflux conditions and Ar for 24 hours. The solvent was removed under reduced pressure and the residue was dissolved in CH_2Cl_2 (100 mL), which was washed with 0.3 M aq. EDTA (2 × 100 mL). After back extraction with CH_2Cl_2 (100 mL), the combined organic phase was washed with brine (100 mL), dried ($MgSO_4$), filtered and concentrated under reduced pressure. The residue was purified by column chromatography (silica gel; CH_2Cl_2–MeOH 5%, v/v) to afford compound **9** as an ochreous yellow solid. Yield 685 mg (47%). Mp 93–100 °C. ^{1}H NMR (DMSO-d_6) δ 3.52–3.75 (m, 5H, OCH_2CHCH_2OH), 4.62 (t, J = 5.55 Hz, 1H, CH_2OH), 4.82 (d, J = 5.10, 1H, $CHOH$), 5.04 (s, 2H, $ArCH_2O$), 7.69–7.84 (m, 3H, Ar), 8.04–8.46 (m, 10H, Ar), 8.65–8.75 (m, 2H, Ar). ^{13}C NMR (DMSO-d_6) δ 63.2 ($CHCH_2OH$), 70.6, 70.7 ($CHCH_2OH$, OCH_2CH), 72.4 ($ArCH_2O$), 93.36, 93.40 ($C{\equiv}C$), 116.8, 120.0, 123.5, 123.8, 124.8, 124.9, 125.1, 125.6, 126.1, 126.2, 126.9, 127.0, 127.3, 127.4, 128.5, 129.1, 130.0, 130.4, 130.6, 130.8, 131.1, 131.2, 132.6, 136.0 (Ar). HR-MALDI-MS calcd for $C_{32}H_{24}O_3Na$ $[M + Na]^+$ m/z 479.1618; found m/z 479.1626.

(*S*)-4-((4-(Pyren-1-ylethynyl)naphthalen-1-yl)methoxy)butane-1,2-diol 10. Compound **10** was synthesized from **8** according to the procedure described for **9**. Yield (80%) bronze coloured foam. ^{1}H NMR ($CDCl_3$) δ 1.72–1.79 (m, 2H, OCH_2CH_2), 2.30, 3.01 (s, 2H, 2 × OH), 3.44–3.50 (m, 1H, $CHCH_2O$), 3.59–3.64 (m, 1H, $CHCH_2O$), 3.74–3.79 (m, 2H, OCH_2CH_2), 3.89–3.92 (m, 1H, CH_2CHCH_2), 4.97, 5.02 (2 × d, J = 12.6 Hz, 2H, $ArCH_2O$), 7.43–7.71 (m, 3H, Ar), 8.88–8.30 (m, 10H, Ar), 8.69–8.76 (m, 2H, Ar). ^{13}C NMR ($CDCl_3$) δ 33.0 (OCH_2CH_2), 66.8 (OCH_2CH_2), 68.5 ($CHCH_2OH$), 71.3 ($CHCH_2OH$), 71.8 ($ArCH_2O$), 93.3, 94.1 ($C{\equiv}C$), 117.9, 122.1, 124.3, 124.7, 125.7, 125.8, 125.8, 126.1, 126.4, 127.0, 127.1, 127.2, 127.4, 128.4, 128.6, 129.9, 130.1, 131.2, 131.4, 131.5, 131.6, 132.0, 132.2, 132.3, 133.6, 134.4 (Ar). HR-MALDI-MS calcd for $C_{33}H_{26}O_3Na$ $[M + Na]^+$ m/z 493.1774; found m/z 493.1782.

(*S*)-1-(Bis(4-methoxyphenyl)(phenyl)methoxy)-3-((4-(pyren-1-ylethynyl)naphthalen-1-yl)-methoxy)propan-2-ol 11. (*R*)-3-((4-(Pyren-1-ylethynyl)naphthalen-1-yl)methoxy)propane-1,2-diol (**9**; 600 mg, 1.314 mmol) was dissolved in dry pyridine (20 mL) and flushed with Ar, before 4,4′-dimethoxytrityl chloride (534mg, 1.577 mmol) dissolved in dry pyridine (10 mL) was added dropwise. The reaction was stirred at room temperature under Ar for 24 h before it was quenched with MeOH (2 mL). The reaction mixture was diluted with CH_2Cl_2–NEt_3 (50 mL, 99.5%/0.5%, v/v) before washed with H_2O (3 × 100 mL). After back extraction with CH_2Cl_2–NEt_3 (50 mL, 99.5%/0.5%, v/v) the combined organic phase was washed with brine (100 mL), dried ($MgSO_4$), filtrated and concentrated under reduced pressure before the residue was purified by column chromatography (silica gel; 0.5% Et_3N v/v, 0–50% EtOAc in cyclohexane) to afford **11** as yellow foam. Yield 895 mg (90%). ^{1}H NMR ($CDCl_3$) δ 3.20–3.23, 3.66–3.76 (2 × m, 5H, OCH_2CH, $CHCH_2O$, $CHCH_2ODMT$), 3.76 (s, 6H, 2 × OMe), 3.99 (br. s, 1H, $CHOH$), 5.02 (s, 2H, $ArCH_2O$), 6.80 (d, J = 6.9 Hz, 4H, DMT), 7.20–7.68 (m, 12H, Ar), 7.88–8.32 (m, 10H, Ar), 8.69–8.76 (m, 2H, Ar). ^{13}C NMR ($CDCl_3$) δ 55.3 (2 × OMe), 64.6 ($CHCH_2ODMT$), 70.2 ($CHCH_2ODMT$, OCH_2CH), 71.8 ($ArCH_2O$), 86.3 (CPh_3), 93.4, 94.0 ($C{\equiv}C$), 113.3, 127.0, 127.4, 128.0, 128.3, 130.2, 136.1, 145.0, 158.6 (DMT), 118.0, 121.8, 124.4, 124.5, 124.7, 124.7, 125.7, 125.8, 126.0, 126.4, 126.9, 127.0, 127.2, 128.4, 128.7, 129.9, 130.1, 131.2, 131.4, 131.5, 131.6,

133.6, 134.7 (Ar). HR-MALDI-MS calcd for $C_{53}H_{42}O_5Na$ [M + Na]$^+$ *m/z* 781.2925; found *m/z* 781.2934.

(*S*)-1-(Bis(4-methoxyphenyl)(phenyl)methoxy)-4-((4-(pyren-1-ylethynyl)naphthalen-1-yl)methoxy)butan-2-ol 12. Compound **12** was synthesized from **10** according to the procedure described for **11**. Yield (58%) bronze coloured foam. ^{1}H NMR ($CDCl_3$) δ 1.82 (m, 2H, OCH_2CH_2), 3.10–3.14, 3.67–3.76 (2 × m, 5H, OCH_2CH_2, $CHCH_2O$, $CHCH_2ODMT$), 3.76 (s, 6H, 2 × OMe), 4.00 (br. s, 1H, CHO*H*), 4.95 (s, 2H, $ArCH_2O$), 6.80 (d, $J = 8.7$ Hz, 4H, DMT), 7.20–7.68 (m, 12H, Ar), 7.87–8.32 (m, 10H, Ar), 8.67–8.78 (m, 2H, Ar). ^{13}C NMR ($CDCl_3$) δ 33.7 (OCH_2CH_2), 55.3 (2 × OMe), 67.4 (OCH_2CH_2), 68.2 ($CHCH_2ODMT$), 69.6 ($CHCH_2ODMT$), 71.6 ($ArCH_2O$), 86.1 (CPh_3), 93.5, 93.9 ($C{\equiv}C$), 113.2, 127.0, 127.4, 128.0, 128.3, 130.2, 136.2, 145.1, 158.6 (DMT), 118.0, 121.8, 124.4, 124.5, 124.7, 125.7, 125.8, 126.4, 127.2, 128.2, 128.4, 128.7, 129.9, 130.1, 131.2, 131.4, 131.5, 131.6, 132.1, 133.6, 134.9 (Ar). HR-MALDI-MS calcd for $C_{54}H_{44}O_5Na$ [M + Na]$^+$ *m/z* 795.3081; found *m/z* 795.3100.

(*S*)-1-(Bis(4-methoxyphenyl)(phenyl)methoxy)-3-((4-(pyren-1-ylethynyl)naphthalen-1-yl)methoxy)propan-2-yl 2-cyanoethyl diisopropylphosphoramidite 13. (*S*)-1-(Bis(4-methoxyphenyl)(phenyl)methoxy)-3-((4-(pyren-1-ylethynyl)naphthalen-1-yl)methoxy)propan-2-ol (**11**; 877 mg, 1.156 mmol) and diisopropyl ammonium tetrazolide (295 mg, 1.723 mmol) were dissolved under Ar in dry CH_2Cl_2 (40 mL), followed by dropwise addition of 2-cyanoethyl *N*,*N*,*N*′,*N*′-tetraisopropylphosphordiamidite (1.097 mg, 3.639 mmol) *via* a syringe at 0 °C. The reaction mixture was stirred under Ar at room temperature overnight before the reaction was quenched with H_2O (50 mL) and the organic phase was washed with H_2O (2 × 50 mL). After back extraction with CH_2Cl_2 (50 mL), the combined organic phase was dried ($MgSO_4$), filtrated and concentrated under reduced pressure. The residue was purified by dry column vacuum chromatography (silica gel; Et_3N 0.5% v/v, 0–50% EtOAc in cyclohexane) to afford **13** as a yellow foam. Yield 996 mg (90%). ^{1}H NMR ($CDCl_3$) δ 1.15 (m, 12H, 2 × $CH(CH_3)_2$), 2.40–2.54 (m, 2H, CH_2CN), 3.21–3.31 (m, 2H, 2 × $CH(CH_3)_2$), 3.55–3.65, 3.67–3.76 (2 × m, 7H, OCH_2CH, $CHCH_2O$, $CHCH_2ODMT$, CH_2CH_2CN), 3.76 (s, 6H, 2 × OMe), 5.00–5.06 (m, 2H, $ArCH_2O$), 6.78 (d, $J = 8.7$ Hz, 4H, DMT), 7.20–7.67 (m, 12H, Ar), 7.86–8.34 (m, 10H, Ar), 8.69–8.80 (m, 2H, Ar). ^{13}C NMR ($CDCl_3$) δ 20.3, 20.4 (CH_2CN), 24.6, 24.7, 24.8, 24.9 (2 × $CH(CH_3)_2$), 43.2, 43.4 (2 × $CH(CH_3)_2$), 55.3 (2 × OMe), 58.4, 58.7 (OCH_2CH_2CN), 64.4 (*C*HOP), 71.6 ($CHCH_2ODMT$), 72.7 (OCH_2CH), 72.9 ($ArCH_2O$), 86.2 (CPh_3), 93.5, 93.9 ($C{\equiv}C$), 113.2, 127.0, 127.4, 127.9, 128.3, 130.2, 136.2, 145.2, 158.6 (DMT), 118.1, 121.6, 124.5, 124.8, 125.7, 125.8, 126.4, 126.9, 126.9, 128.4, 128.7, 129.9, 130.1, 130.3, 131.2, 131.4, 131.5, 132.1, 133.5, 135.0, 135.2, 136.3, 136.3 (Ar). ^{31}P NMR ($CDCl_3$): δ 150.3, 150.4. HR-MALDI-MS calcd for $C_{62}H_{59}N_2O_6PNa$ [M + Na]$^+$ *m/z* 981.4004; found *m/z* 981.3995.

(*S*)-1-(Bis(4-methoxyphenyl)(phenyl)methoxy)-4-((4-(pyren-1-ylethynyl)naphthalen-1-yl)methoxy)butan-2-yl 2-cyanoethyl diisopropylphosphoramidite 14. Compound **14** was synthesized from **12** according to the procedure described for **13**. Yield (81%) yellow foam. ^{1}H NMR ($CDCl_3$) δ 1.16 (m, 12H, 2 × $CH(CH_3)_2$), 1.92–2.04 (m, 2H, OCH_2CH_2), 2.49–2.56 (m, 2H, CH_2CN), 3.48–3.73 (m, 2H, 2 × $CH(CH_3)_2$), 3.55–3.76 (m, 7H, OCH_2CH_2, $CHCH_2O$, $CHCH_2ODMT$, CH_2CH_2CN), 3.76 (s, 6H, 2 × OMe), 4.93, 4.97 (m, 2H, $ArCH_2O$), 6.76–6.81 (m, 4H, DMT), 7.17–7.71 (m, 12H, Ar), 7.86–8.33 (m, 10H, Ar), 8.69–8.80 (m, 2H, Ar). ^{13}C NMR ($CDCl_3$) δ 20.3 (CH_2CN), 24.5, 24.6, 24.7, 24.8 (2 × $CH(CH_3)_2$), 34.1 (OCH_2CH_2), 43.1, 43.2 (2 × $CH(CH_3)_2$), 55.3 (2 × OMe), 58.2 (OCH_2CH_2CN), 66.4 (*C*HOP), 67.1 (OCH_2CH_2), 71.3 ($CHCH_2ODMT$), 71.3 ($ArCH_2O$), 86.0 (CPh_3), 93.5, 93.9 ($C{\equiv}C$), 113.1, 127.1, 127.4, 127.9, 128.4, 130.3, 136.4, 145.2, 158.5 (DMT), 118.1, 124.5, 124.6, 124.8, 125.7, 125.8, 126.4, 126.8, 126.8, 126.9, 128.4, 128.7, 129.9, 130.2, 131.3, 131.4, 131.5, 131.7, 133.6, 135.3, 135.4, 136.5 (Ar). ^{31}P NMR ($CDCl_3$): δ 149.6, 150.0. HR-MALDI-MS calcd for $C_{63}H_{61}N_2O_6PNa$ [M + Na]$^+$ *m/z* 995.4160; found *m/z* 995.4145.

(*S*)-4-(4-Iodophenoxy)butane-1,2-diol 15. An ice-cooled solution of diethyl azodicarboxylate (DEAD, 2.42 ml, 15.6 mmol) in THF (150 ml) was treated with 2-(2,2-dimethyl-1,3-dioxolan-4-yl)ethanol (**6**, 1.84 ml, 12.95 mmol) for 25 min before 4-iodophenol (3.70 g, 16.8 mmol), and PPh_3 (4.08 g, 15.6 mmol) were added. After 45 min at 0 °C, the reaction mixture was allowed to reach room temperature overnight. The reaction was quenched with saturated aq. NH_4OH (100 ml) and the mixture was extracted with EtOAc. The organic layer was washed with water, dried ($MgSO_4$), and concentrated under reduced pressure. The residue was purified by column chromatography (silica gel; petroleum ether (60–80 °C)–Et_2O, 1 : 1, v/v) to afford (*S*)-4-(2-(4-iodophenoxy)ethyl-2,2-dimethyl-1,3-dioxolane as an oil. Yield 2.87 g (72%). ^{1}H NMR ($CDCl_3$) δ 1.36, 1.42 (2 s, 6H, $C(CH_3)_2$), 2.04 (q, $J = 6.3$ Hz, 2H, OCH_2CH_2), 3.63 (t, $J = 7.8$ Hz, 1H, OC*H*HCH), 4.02–4.13 (m, 3H, $OCHHCH_2$, OCH_2CHCH_2), 4.28 (quintet, $J = 6.3$ Hz, 1H, OCH_2CHCH_2), 6.69 (d, $J = 9.0$ Hz, 2H, Ar), 7.54 (d, $J = 9.0$ Hz, 2H, Ar). ^{13}C NMR ($CDCl_3$) δ 25.7, 26.9 (2 × $C(CH_3)_2$), 33.4 (OCH_2CH_2), 64.8 (OCH_2CH_2), 69.5 (CH_2CHCH_2), 73.3 (CH_2CHCH_2), 82.8 (Ph), 108.9 ($C(CH_3)_2$), 116.9, 138.2 (Ph), 158.6 (Ph). HR-MALDI-MS calcd for $C_{13}H_{17}IO_3Na$ [M + Na]$^+$ *m/z* 371.0115; found *m/z* 371.0112. (*S*)-4-(2-(4-Iodophenoxy)ethyl)-2,2-dimethyl-1,3-dioxolane (1.2 g, 5.75 mmol) was treated with 80% aq. AcOH (25 ml) for 24 h at room temperature. The solvent was removed under reduced pressure and the residue was coevaporated with toluene–EtOH (2 × 30 ml, 5 : 1, v/v). The residue was dried under reduced pressure to afford **15** as an oil, which was used in the next step without further purification. Yield 1.73 g (98%). ^{1}H NMR (DMSO-d_6) δ 1.58–1.67 (m, 1H, OCH_2CHH), 1.87–1.96 (m, 1H, OCH_2CHH), 3.26–3.67 (m, 2H, $CHCH_2OH$), 3.60–3.64 (m, 1H, $CHCH_2OH$), 4.05 (t, $J = 6.8$ Hz, 2H, OCH_2CH_2), 4.54 (t, $J = 5.6$ Hz, 1H, $CHCH_2OH$), 4.60 (d, $J = 5.4$ Hz, 1H, CH_2CHOH), 6.78 (d, $J = 9.0$ Hz, 2H, Ph), 7.57 (d, $J = 9.0$ Hz, 2H, Ph). ^{13}C NMR (DMSO-d_6) δ 32.9 (OCH_2CH_2), 64.7 (OCH_2CH_2), 65.9 (CH_2CHOH), 67.9 (CH_2OH), 82.7 (Ph), 117.2, 137.8 (Ph), 158.5 (Ph). HR-MALDI-MS calcd for $C_{10}H_{13}IO_3$ [M + Na]$^+$ *m/z* 330.9802; found *m/z* 330.9793.

(*S*)-4-(4-(Pyren-1-ylethynyl)phenoxy)butane-1,2-diol 16. (*S*)-4-(4-Iodophenoxy)butane-1,2-diol (**15**; 1.00 g, 3.24 mmol), $Pd(PPh_3)_2Cl_2$ (161 mg, 0.23 mmol) and CuI (72 mg, 0.38 mmol) were dissolved in dry NEt_3 (40 ml). The mixture was flushed with Ar for 10 minutes before 1-ethynylpyrene (1.086 g, 4.80 mmol) was added. The reaction mixture was stirred for 24 hours. The solvent was removed under reduced pressure and the residue was dissolved in CH_2Cl_2 (100 ml), which was washed with 0.3 M aq.

EDTA (2 × 100 ml). After back extraction with CH_2Cl_2 (100 ml), the combined organic phase was washed with brine (100 ml), dried ($MgSO_4$), filtered and concentrated under reduced pressure. The residue was purified by column chromatography (silica gel; 5% MeOH in CH_2Cl_2, v/v) to afford compound **16** as yellow solid. Yield 1.17 g (74%). Mp 171–173 °C. ^{1}H NMR (DMSO-d_6) δ 1.65–1.76 (m, 1H, OCH_2CHH), 1.94–2.05 (m, 1H, OCH_2CHH), 3.37–3.45 (m, 2H, $CHCH_2OH$), 3.67–3.73 (m, 1H, $CHCH_2OH$), 4.18 (t, J = 6.7 Hz, 2H, OCH_2CH_2), 4.61 (t, J = 5.7 Hz, 1H, $CHCH_2OH$), 4.68 (d, J = 5.41 Hz, 1H, CH_2CHOH), 7.07 (d, J = 9.0 Hz, 2H, Ar), 7.70 (d, J = 9.0 Hz, 2H, Ar), 8.11–8.39 (m, 8H, Ar), 8.63 (d, J = 9.0 Hz, 1H, Ar). ^{13}C NMR (DMSO-d_6) δ 33.0 (OCH_2CH_2), 64.8 (OCH_2CH_2), 65.9 (CH_2CHOH), 67.9 (CH_2OH), 86.8, 95.5 ($C{\equiv}C$), 114.1, 114.9, 117.2, 123.4, 123.6, 124.8, 125.8, 125.8, 126.6, 127.2, 128.1, 128.6, 129.3, 130.5, 130.6, 130.7, 130.8, 133.1, 159.2 (Ar). HR-MALDI-MS calcd for $C_{28}H_{22}O_3$ $[M]^+$ m/z 406.1564; found m/z 406.1560

(*S*)-1-(Bis(4-methoxyphenyl)(phenyl)methoxy)-4-(4-(pyren-1-ylethynyl)phenoxy)butane-2-ol 17. (*S*)-4-(4-(Pyren-1-ylethynyl)-phenoxy)butane-1,2-diol (**16**; 0.745 g, 1.83 mmol) was dissolved in dry pyridine (20 ml) before 4,4′-dimethoxytrityl chloride (0.743 g, 2.20 mmol) was added under N_2. The reaction was stirred at room temperature overnight before it was quenched with MeOH (2 ml). The reaction mixture was diluted with EtOAc (150 ml) before washing with saturated aq. $NaHCO_3$ (2 × 40 ml). After back extraction with EtOAc (2 × 20 ml), the combined organic phase was dried (Na_2SO_4), filtered, and concentrated under reduced pressure. The residue was coevaporated with toluene–EtOH (2 × 25 ml, 1 : 1, v/v) before it was purified by column chromatography (silica gel; 0.5% Et_3N v/v, 20–50% EtOAc in cyclohexane) to afford **17** as a yellow foam. Yield 1.27 g (98%). ^{1}H NMR (DMSO-d_6) δ 1.60–1.71 (m, 1H, OCH_2CHH), 1.90–1.97 (m, 1H, OCH_2CHH), 2.48 (br. s, 1H, ($CHOH$), 3.13–3.29 (m, 2H, CH_2ODMT), 3.79 (s, 6H, 2 × OCH_3), 4.02–4.15 (m, 3H, OCH_2CH_2, CH_2CHCH_2), 6.83 (d, J = 9.0 Hz, 4H, DMT), 6.89 (d, J = 8.7 Hz, 2H, Ar), 7.20–7.34 (m, 7H, Ar), 7.44 (d, J = 8.1 Hz, 2H, Ar) 7.62 (d, J = 9.0 Hz, 2H, Ar), 7.98–8.22 (m, 8H, Ar), 8.65 (d, J = 9.3 Hz, 1H, Ar). ^{13}C NMR ($CDCl_3$) δ 33.0 (OCH_2CH_2), 55.2 (2 × OCH_3), 64.9 (OCH_2CH_2), 67.4 (CH_2CHOH), 68.4 (CH_2ODMT), 86.2 (CPh_3), 87.3, 95.2 ($C{\equiv}C$), 113.6, 114.7, 115.6, 118.2, 124.4, 124.5, 125.5, 125.5, 125.6, 126.2, 126.9, 127.3, 127.8, 127.9, 127.9, 128.1, 128.2, 129.4, 130.1, 131.0, 133.1, 131.3, 131.7, 133.1, 135.9, 158.5, 159.0 (Ar). HR-ESI-MS calcd for $C_{49}H_{40}O_5Na$ $[M + Na]^+$ m/z 731.2768; found m/z 731.2751.

(*S*)-1-(Bis(4-methoxyphenyl(phenyl)methoxy)-4-(4-(pyren-1-yl-ethynyl)phenoxy)butan-2-yl) 2-cyanoethyl diisopropylphospho-ramidite 18. Compound **18** was synthesized from **17** according to the procedure described for **13**. Yield (85%) yellow foam. ^{31}P NMR ($CDCl_3$) δ 149.7, 150.1. HR-ESI-MS calcd for $C_{58}H_{57}N_2NaO_6P^+$ $[M + Na]^+$ m/z 931.3848; found m/z 931.3870.

Synthesis and purification of modified oligonucleotides

Modified oligonucleotides were synthesized on a 0.2 μmol scale on 500 Å CPG supports using an Expedite Nucleic Acid Synthesis System Model 8909 (Applied Biosystems). Standard procedures were used for the coupling of commercial phosphoramidites whereas modified phosphoramidites were coupled with 1*H*-tetrazole as an activator with an extended coupling time (10 min). DMT-on ONs were cleaved from the CPG-support with 32% aqueous ammonia (1.2 mL) and were deprotected at 55 °C overnight. Purification of ONs was carried out on reverse-phase semipreparative HPLC on a Waters Xterra MS C_{18} column (10 μm, 7.8 mm × 150 mm). DMT deprotection was done with 80% aq. AcOH (100 μL) for 20 minutes, followed by addition of H_2O (100 μL) and 3 M aq. NaOAc (50 μL). The ONs were precipitated from 99.9% EtOH (550 μL) at –18 °C. The purity of the obtained ONs was checked by ion-exchange chromatography on a LaChrom system (Merck Hitachi) using a GenPak-Fax column (Waters), see ESI.† Verification was done by MALDI-TOF analysis on a Voyager Elite Bio spectrometry Research Station (Perspective Biosystems), Table 3.

Table 3 Calculated and found masses of synthesized oligonucleotides

		m/z (Da)	
Entry	Sequence	Calcd.	Found[a]
ON3	5′-CCCCTT**2**TCTTTTTT	4640.3	4642.1
ON4	5′-CCCCTT**3**TCTTTTTT	4654.3	4651.1
ON5	5′-CCCCTT**4**TCTTTTTT	**4589.2**	**4586.4**
ON7	5′-CCCCTT**2**TCT**2**TTTTT	5158.8	5158.4
ON8	5′-CCCCTT**3**TCT**3**TTTTT	5186.8	5185.6
ON9	5′-CCCCTT**4**TCT**4**TTTTT	**5056.6**	5053.3
ON10	5′-CCCCT**2**TTCTT**2**TTTT	5158.8	5153.2

[a] Measured by MALDI-TOF MS.

Melting temperature measurements

T_m measurements were performed on a PerkinElmer Lambda 35 UV/VIS spectrometer with a PTP 6 thermostat and PerkinElmer Templab 2.00 software. Triplexes were formed by mixing 1.0 μM of each ssDNA and 1.5 μM of the TFO in the corresponding buffer solution and duplexes were formed by mixing 1.0 μM of each ONs. The solutions were heated to 80 °C for 5 min and afterward cooled to 4 °C and kept at this temperature for 30 minutes. The absorbance of triplexes/duplexes was measured at 260 nm or 373 nm from 5 °C to 80 °C with a heating rate of 1.0 °C min^{-1}. The melting temperatures (T_m, °C) were determined as the maximum of the first derivative plots of the melting curves. All melting temperatures are within the uncertainty ±0.5 °C.

Acknowledgements

The Nucleic Acid Center is funded by The Danish National Research Foundation for studies on nucleic acid chemical biology. This work was supported by the Sixth Framework Program Marie Curie Host Fellowships for Early Stage Research Training under contract number MEST-CT-2004-504018.

References

1 K. M. Vasquez and P. M. Glazer, *Q. Rev. Biophys.*, 2002, **35**, 89–107.
2 J. Y. Chin, E. B. Schleifman and P. M. Glazer, *Front. Biosci.*, 2007, **12**, 4288–4297.
3 M. Faria and C. Giovannangeli, *J. Gene Med.*, 2001, **3**, 299–310.
4 S. Buchini and C. J. Leumann, *Curr. Opin. Chem. Biol.*, 2003, **7**, 717–726.
5 K. R. Fox, *Curr. Med. Chem.*, 2000, **7**, 17–37.

6 T. Højland, S. Kumar, B. R. Babu, T. Umemoto, N. Albæk, P. K. Sharma, P. Nielsen and J. Wengel, *Org. Biomol. Chem.*, 2007, **5**, 2375–2379.
7 V. V. Filichev, M. C. Nielsen, N. Bomholt, C. H. Jessen and E. B. Pedersen, *Angew. Chem., Int. Ed.*, 2006, **45**, 5311–5315.
8 C. H. Jessen and E. B. Pedersen, *Helv. Chim. Acta*, 2004, **87**, 2465–2471.
9 K. R. Fox and T. Brown, *Q. Rev. Biophys.*, 2005, **38**, 311–320.
10 V. V. Filichev and E. B. Pedersen, *J. Am. Chem. Soc.*, 2005, **127**, 14849–14858.
11 M. Paramavisam, C. Susanna, V. V. Filichev, N. Bomholt, E. B. Pedersen and L. E. Xodo, *Nucleic Acids Res.*, 2008, **36**, 3494–3507.
12 I. Géci, V. V. Filichev and E. B. Pedersen, *Bioconjugate Chem.*, 2006, **17**, 950–957.
13 V. V. Filichev, H. Gaber, T. R. Olsen, P. T. Jørgensen, C. H. Jessen and E. B. Pedersen, *Eur. J. Org. Chem.*, 2006, 3960–3968.
14 I. Géci, V. V. Filichev and E. B. Pedersen, *Chem.–Eur. J.*, 2007, **13**, 6379–6386.
15 D. Globisch, N. Bomholt, V. V. Filichev and E. B. Pedersen, *Helv. Chim. Acta*, 2008, **91**, 805–818.
16 B. C. Froehler, S. Wadwani, T. J. Terhorst and S. R. Gerrard, *Tetrahedron Lett.*, 1992, **33**, 5307.
17 J.-L. Mergny and L. Lacroix, *Oligonucleotides*, 2003, **13**, 515–537.